110, 215 (1983).
3. H. Nakane, M. Nakayama, T. Ayabe, T. Nishimura, and T. Kimura, in "Proceedings of Semiconductors and Integrated Circuits Technology," Vol. 1, p. 571 (1978).
4. M. K. Lee, C. Y. Lu, and C. T. Shih, *This Journal,* **130,** 2249 (1983).
5. D. E. Clark, C. G. Pantano, Jr., and L. L. Hench, "Corrosion of Glass," Magazines for Industry, New York (1979).
6. W. A. Pliskin and H. S. Lehman, *This Journal,* **112,** 1013 (1965).
7. W. A. Pliskin, *J. Vac. Sci. Technol.,* **14,** 1064 (1977).
8. R. J. H. Lin, J. C. Lee, and P. B. Zimmer, ALO-5300-T2, U.S. Department of Energy, Washington, DC (1979).

Etching of Tungsten and Tungsten Silicide Films by Chlorine Atoms

D. S. Fischl,*[,1] G. W. Rodrigues,[2] and D. W. Hess**

Department of Chemical Engineering, University of California, Berkeley, California 94720

ABSTRACT

Thin films of tungsten and tungsten silicide were etched both within and downstream from a Cl_2 plasma discharge at 200 mtorr pressure and temperatures below 150°C. When samples were positioned downstream from the discharge, etching proceeded solely by chemical reaction of the film with chlorine atoms. Without a discharge, molecular chlorine did not etch tungsten or tungsten silicide. Downstream and in-plasma tungsten etch rates were approximately equal at 110°C, but the chlorine atom etch rate dropped more rapidly than the in-plasma etch rate as temperature decreased. The chemical reaction between chlorine atoms and the tungsten film was proportional to the gas phase Cl atom mole fraction. A pretreatment consisting of either a dilute hydrofluoric acid dip or a short plasma etch cycle was necessary for atom etching of tungsten silicide films. The etch rates of tungsten silicide in Cl_2 plasmas were approximately an order of magnitude higher and less temperature sensitive than those in the downstream (atom) configuration.

The patterning of tungsten and tungsten silicide for microelectronic circuits has been accomplished by a variety of halogen-based dry processing etching techniques (1-8). Publications on the patterning of these materials using chlorine have only summarized the effects that the process parameters have on the anisotropy, etch rate, and selectivity (5). The limited results suggest that the etch rate of tungsten is related to the concentration of chlorine atoms, Cl, produced by either laser irradiation (8) or gas-phase electron impact dissociation (5) of molecular chlorine, Cl_2. However, the etching process was controlled empirically and thus is not based on a fundamental understanding of the etching mechanism.

Control of thin film etching processes during microelectronic device manufacture is often difficult. In large part, the difficulties arise from the complexity of RF glow discharges, coupled with plasma-film interactions. One method of simplifying the etch chemistry of these processes is to utilize an upstream discharge to generate reactive atoms for etching. Since ion, electron, and photon bombardment are absent in this configuration, the pure atom etch chemistry can be studied. Comparison of downstream etching with in-plasma or discharge etching then generates insight into the role of the plasma. Furthermore, such investigations yield fundamental information concerning atom reactions with materials. In this paper we present results on the chlorine atom etching (downstream or flowing afterglow reactor configuration) and Cl_2 discharge etching of tungsten and tungsten silicide thin films.

Experimental

The reactor used for plasma etching (in the discharge) has been described in an earlier publication (5). The flow reactor was modified for atom etching by connecting a discharge and flow tube upstream from the etching reactor. A schematic of the system can be found in Ref. (9).

An upstream RF discharge was used to dissociate Cl_2 molecules into Cl atoms, which then passed through a flow tube into the reactor where they reacted chemically with tungsten or tungsten silicide samples without the influence of the discharge. Power was supplied by a Tegal Corporation 300W RF generator and matching network to the upstream discharge via two 1.0 cm wide copper bands that were placed around the 3.8 cm diam quartz discharge tube. Spacing between the bands was 1.0 cm. A metal box enclosed the discharge area to ensure RF shielding and to facilitate forced air cooling of the tube. The 3.8 cm diam Pyrex flow tube contained two 90° bends to prevent light from the upstream discharge from reaching the reactor and thus the photomultiplier tube. The flow tube was coated with Halocarbon Corporation 1200 wax to minimize recombination of Cl atoms. The tubes and reactor were connected using MDC Corporation glass to metal Kwik-Flange adapters.

Samples were placed inside the 2.6 liter Pyrex reactor chamber on a temperature controlled 2.5 cm diam anodized aluminum rod that served as the lower electrode for plasma etching experiments. Rod temperature was varied from 25° to 150°C using heating tape and an Omega Engineering Incorporated Model 650/660 controller. In order to reduce the surface area for atom recombination and thus increase the atom concentration at the sample surface, the upper electrode was removed during tungsten atom etching experiments.

Molecular and atomic chlorine traveled approximately 60 cm from the discharge section to the sample location. The chlorine flow rate was controlled by a needle valve and measured with a rotameter. Vacuum was provided by a liquid nitrogen cold trap and a Busch Corporation Lotos corrosion resistant mechanical pump. The pressure in the reactor (200 mtorr) was established by a throttling valve at the exit from the reactor and was monitored by a capacitance manometer.

The gas phase chlorine atom concentration at the position of the sample was measured by titration with nitrosyl chloride (10-13). The NOCl titrant (Matheson) entered the reactor approximately 7 cm upstream from the sample location through a manifold to disperse gas evenly throughout the flow cross section. Flow rate was regulated by a needle valve and measured with a Tylan FM 360 mass flowmeter. Monel and Teflon were the materials used for the NOCl delivery system. A Hamamatsu R1928 photomultiplier tube with a Melles Griot 03FIV008 filter was used to monitor the 550 nm emission (chemiluminescence) resulting from the recombination reaction of chlorine atoms (9,

*Electrochemical Society Student Member.
**Electrochemical Society Active Member.

DOCKET ALARM Find authenticated court documents without watermarks at docketalarm.com.

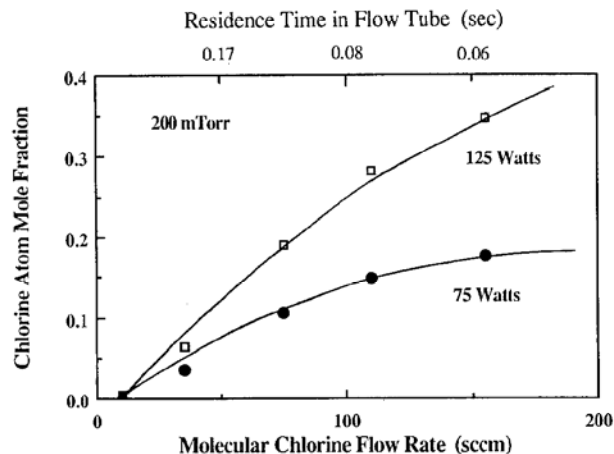

Fig. 1. Effect of Cl_2 flow rate on the atom yield in the reactor at 200 mtorr total pressure and for two different powers to the upstream discharge.

Chemical vapor deposition was used to form the 250 nm thick tungsten silicide films which had a resistivity of 1000 μΩ-cm, and an approximate Si/W ratio of 2.5. Both film types were deposited onto oxidized silicon wafers, which were then broken into samples of approximately 1 cm^2 [details of film preparation can be found in Ref. (5)]. Etch rates were determined from the film thickness and the time required for the film to visually clear from the oxide surface.

Results

Chlorine atoms.—Molecular chlorine gas, Cl_2, is partially dissociated into Cl atoms by the upstream plasma. These atoms then travel through the flow tube to the reactor with some of them recombining by third body (*e.g.*, Cl_2 or wall) collisions. The concentration of gas-phase chlorine atoms in the reactor at the location of the sample is varied by changing the Cl_2 flow rate and the upstream discharge power. Titration results yield a linear relationship between the Cl atom concentration and the square root of the chemiluminescence intensity (13-15). The Cl atom concentration is then easily determined by measurement of the intensity. Since all experiments are performed at a constant pressure of 200 mtorr, results are presented in terms of the chlorine atom mole fraction.

The effect of chlorine flow rate on the atom yield in the reactor is shown in Fig. 1. At constant RF power, a fixed amount of Cl_2 is dissociated in the upstream discharge. The number of atoms that recombine while traveling to the reactor depends on the flow rate, pressure, and recombination kinetics. These data show that the chlorine atom mole fraction increases with an increase in flow rate at constant pressure. This behavior is consistent with a decrease in gas residence time at higher flow rates since shorter residence times mean that more of the atoms produced in the discharge arrive at the reactor before recombining (16). However, the atom mole fraction levels off at higher flow rates because, at constant power, the number of atoms produced decreases when the residence time in the upstream discharge becomes too short. Figure 1 also shows that an increase in power to the upstream discharge increases the chlorine atom mole fraction. This effect is due to increased electron impact dissociation of chlorine molecules.

Figure 2 shows the effect of increasing the RF power to the upstream discharge at a constant flow rate of 100 sccm Cl_2 and a pressure of 200 mtorr. As expected, an increase in power produces an increase in the Cl atom fraction. At 100W, one-third of the molecular chlorine molecules that enter the system remain dissociated when they arrive at the sample location. The data shown in Fig. 2 emphasize the fact that molecular dissociation is not linearly related to the applied discharge power.

Tungsten etching.—The effect of temperature on the tungsten etch rate at a pressure of 200 mtorr and a total gas flow rate of 100 sccm is shown in Fig. 3. Solid symbols represent data from plasma etching experiments (5), where the sample is positioned within the discharge and subjected to ion bombardment. The open squares are results from the current study, where etching of the tungsten film is solely due to chemical reaction with chlorine atoms. For these data points, the gas-phase mole fraction of chlorine atoms, Cl, is 0.5. Without an upstream or *in situ* discharge, no reaction of tungsten occurs with chlorine molecules, Cl_2, at temperatures up to 150°C. However, it should be mentioned that thermal dissociation of chlorine molecules and subsequent reaction with tungsten occurs at surface temperatures above 600°C (8, 17). As the temperature is reduced, etch rates fall and the rate enhancement by ion bombardment is greater than at higher temperatures. The atom and plasma etch rates are approximately equal at 110°C. Obviously, in plasma etching, the etch rate is not critically dependent on thermal heating which is a controlling factor in atom etching. In the case of plasma etching, ion bombardment from the discharge supplies energy to break bonds as well as heat the surface. However, experiments using thermally bonded samples have shown that plasma heating does not significantly affect the tungsten etch rate (5). If an Arrhenius temperature dependence is assumed, the apparent activation energies of the reactions are 0.1 and 0.3 eV/molecule for plasma etching and atom etching, respectively.

It was shown in Fig. 2 that the atom concentration in the reactor can be varied by changing the upstream discharge power. This fact is used to quantitatively determine the effect of the gas-phase chlorine atom concentration on the tungsten etch rate. The data in Fig. 4 are from experiments at three different temperatures with the flow rate and the pressure constant at 100 sccm and 200 mtorr, respectively. At these temperatures, the etch rate varies linearly with the gas-phase chlorine atom mole fraction. The solid lines depict the best fit for all data and are described by

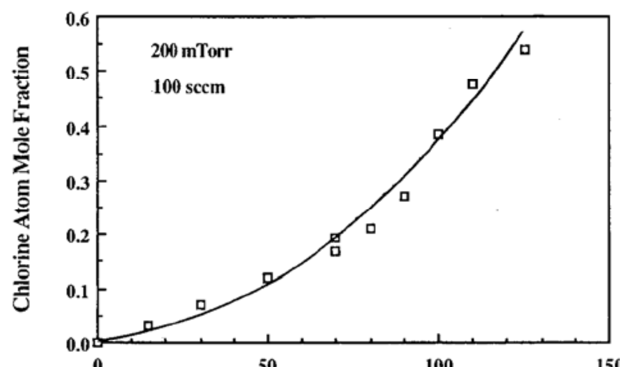

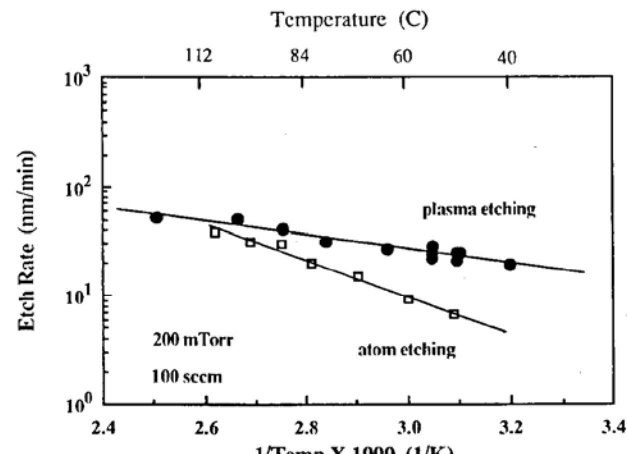

DOCKET ALARM
Find authenticated court documents without watermarks at docketalarm.com.

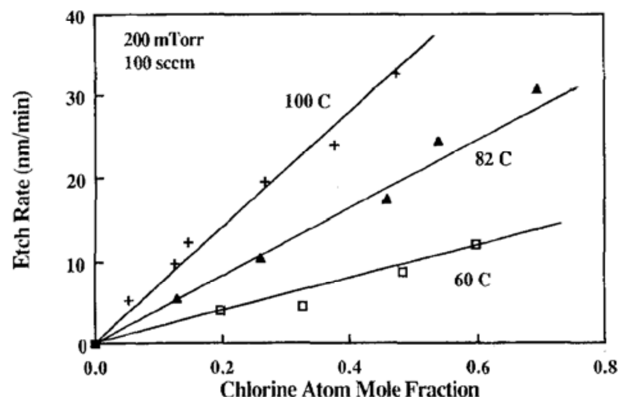

Fig. 4. Effect of chlorine atom mole fraction on the tungsten etch rate at 200 mtorr pressure, 100 sccm Cl_2 flow, and three different rod temperatures.

$$\text{Etch rate [nm/min]} = 2.3 \times 10^6\ X_{Cl} \exp(-3900/T)$$

where X_{Cl} is the chlorine atom mole fraction in the gas-phase and T is the anodized aluminum rod temperature in Kelvin. The pre-exponential constant in the equation does not change with flow rate over the range of 20-150 sccm. This observation indicates that the reaction is not limited by a mass-transport boundary layer. At 200 mtorr pressure and $X_{Cl} = 0.5$, kinetic theory predicts that approximately 10^{19} chlorine atoms strike a square centimeter of surface per second. An etch rate of 40 nm/min requires that approximately 10^{15} tungsten atoms leave a square centimeter of surface per second. If the etch product is assumed to be WCl_4, the reaction probability of Cl atoms is approximately 10^{-4}. This is the predominate product detected by ultrahigh vacuum experiments with molecular and atomic chlorine beams and is also the product predicted by evaluation of equilibrium vapor pressures of the possible tungsten chloride products at these temperatures (17).

Tungsten silicide etching.—Unlike tungsten, tungsten silicide that is exposed to air for longer than a few days does not etch spontaneously with chlorine atoms. However, if the samples are first dipped in a 5% HF solution or subjected to a Cl_2 plasma discharge they can be etched downstream by chlorine atoms. Apparently, ion bombardment is necessary to remove the silicon dioxide layer that forms on the surface of the samples during exposure to air at room temperature. Therefore, tungsten silicide is etched by chlorine atoms by first subjecting the samples to a Cl_2 discharge for 30s (200 mtorr, 150 sccm total gas flow, 10W), which is the shortest time found to ensure complete removal of the native oxide layers. The amount of material removed during the 30s is calculated based on plasma etching experiments at the same temperature and the remaining film thickness is used in the atom etch rate calculation. Althouugh this procedure is not ideal, the error is small. Furthermore, the etch rates calculated in this manner are in agreement with the rates obtained by using an HF dip prior to the etch run. Because exposure to air results in the growth of an oxide film on the WSi_x surface, the upper electrode used for the plasma etch remains in place during the atom experiments. This electrode offers additional surface area for Cl atom recombination compared to the electrode configuration for the tungsten etching experiments. Chlorine atom concentrations are thus lower than observed for identical upstream discharge studies when etching tungsten (compare Fig. 4 and 6). The plasma pretreatment is preferred over the HF dip because the film clears more uniformly and the endpoint is easier to observe. Without a discharge, tungsten silicide did not etch in molecular chlorine under the conditions investigated.

The effect of temperature on the etch rate of tungsten silicide films in the discharge and by Cl atoms is shown in Fig. 5, where the data are obtained at 200 mtorr and 150 sccm Cl_2 flow rate. The solid symbols are the plasma etching results and the open symbols are the Cl atom etching results with a Cl mole fraction of 0.2. Clearly, tungsten silicide is etched by Cl atoms, but at a much slower rate than that obtained in the discharge when ion bombardment occurs. However, the relatively low atom concentrations could also be a major cause of the reduced etch rates in the downstream configuration.

Similar to the tungsten etching results shown in Fig. 3, plasma etch rates of tungsten silicide are less temperature dependent than atom etch rates. The apparent activation energies calculated from the data in Fig. 5 are 0.06 and 0.16 eV/molecule for plasma etching and atom etching, respectively.

The etch rate of silicon is known to be greatly enhanced by ion bombardment in Cl_2 discharges (18, 19). Furthermore, preliminary investigations in our laboratory indicate that heavily doped (approximately 10^{20} cm^{-3}) n^+ polysilicon films are etched by Cl atoms (downstream configuration) at comparable rates to those observed for W and WSi_x. Therefore, the large etch rate enhancement due to the discharge and the magnitude of the atom etch rate suggest that the overall etching process of tungsten silicide is limited by the presence of silicon in the film. Whether this observation is due to volatility considerations, a reduction in electron concentration in the solid (resulting in lowered etchant adsorption), or the fact that the strong (1.8 eV) Si—Si bond is essentially eliminated in the silicide films is not clear at this time.

The variation of WSi_x etch rate with the limited range of chlorine atom mole fractions achieved is shown in Fig. 6 for 100°C, 200 mtorr, and 150 sccm. Again, the etch rate increases with an increase in the Cl-atom mole fraction. Unfortunately, because of the limited range of chlorine atom concentrations that could be obtained with our apparatus, a general kinetic expression describing atom etching of the tungsten silicide films was not formulated.

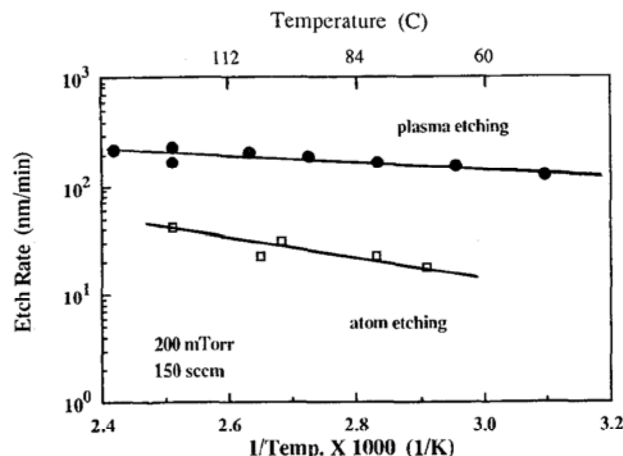

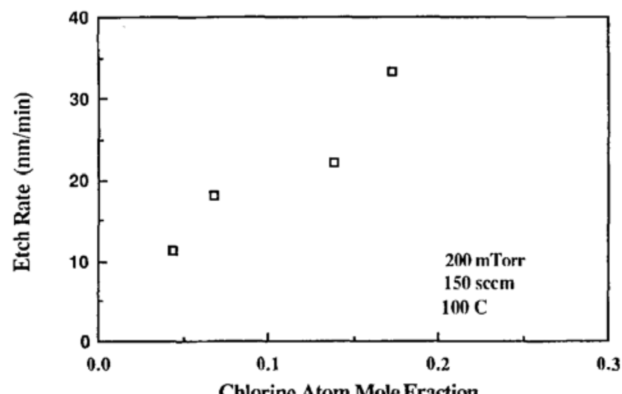

DOCKET ALARM
Find authenticated court documents without watermarks at docketalarm.com.

Conclusions

Tungsten and tungsten silicide thin films have been etched both by Cl_2 plasma discharges and by Cl atoms without the influence of the plasma. Molecular chlorine did not etch the films at the temperatures investigated. Both films could be etched by atomic chlorine, however, a native oxide layer present on tungsten silicide had to be removed before the atoms could attack the film. The results show that plasma interactions greatly enhance the Cl atom etch rate of tungsten silicide. However for tungsten, the etching process proceeds mainly by chemical reaction of the film with Cl atoms and is less affected by the plasma.

Acknowledgments

The authors thank P. Marmillion at IBM Essex Junction, Vermont for supplying the tungsten and tungsten silicide samples used in this investigation. The corrosion resistant pump was supplied by Busch Incorporated, Virginia Beach, Virginia and maintained by Semivac Corporation in Milpitas, California. This work was funded by Intel Corporation and the California State MICRO program.

Manuscript submitted Oct. 9, 1987; revised manuscript received Jan. 18, 1988.

REFERENCES

1. S. P. Murarka, *Solid State Technol.*, 181 (Sept. 1985); S. P. Murarka, "Silicides for VLSI Applications," Academic Press, Inc., Orlando, FL (1983).
2. Y. Pauleau, *Solid State Technol.*, 61 (Feb., 1987); R. S. Blewer, *ibid.*, 117 (Nov. 1986).
3. T. P. Chow and A. J. Steckl, *This Journal*, **131**, 2325 (1984).
4. Workshop on Tungsten and Other Refractory Metals for VLSI Applications, Continuing Education in Engineering, University Extension, University of California, Berkeley, Palo Alto, CA, Nov. 12-14, 1986.
5. D. S. Fischl and D. W. Hess, *This Journal*, **134**, 2265 (1987).
6. G. Koren, *Appl. Phys. Lett.*, **47**, 1012 (1985).
7. M. Rothschild, J. H. C. Sedlacek, and D. J. Ehrlich, *ibid.*, **49**, 1554 (1986).
8. M. Rothschild, J. H. C. Sedlacek, J. G. Black, and D. J. Ehrlich, *J. Vac. Sci. Technol. B*, **5**, 414 (1987).
9. D. A. Danner and D. W. Hess, *J. Appl. Phys.*, **59**, 940 (1986).
10. M. A. A. Clyne and W. S. Nip, in "Reactive Intermediates in the Gas Phase," by D. W. Setser, Editor, Chap. 1, Academic Press, Inc. (1979).
11. M. A. A. Clyne, H. W. Cruse, and R. T. Watson, *J. Chem. Soc., Faraday Trans. II*, **68**, 153 (1972).
12. M. A. A. Clyne and H. W. Cruse, *ibid.*, **68**, 1281 (1972).
13. M. A. A. Clyne and D. H. Stedman, *Trans. Faraday Soc.*, **64**, 1816 (1968).
14. M. A. A. Clyne and D. H. Stedman, *ibid.*, **64**, 2698 (1968).
15. M. A. A. Clyne and D. J. Smith, *J. Chem. Soc., Faraday Trans. 2*, **75**, 704 (1979).
16. C. G. Hill, "An Introduction to Chemical Engineering Kinetics and Reactor Design," p. 262, John Wiley and Sons, Inc., New York (1977).
17. M. Balooch, D. S. Fischl, D. R. Olander, and W. J. Siekhaus, *This Journal*, **135**, 0000 (1988).
18. S. C. McNevin and G. E. Berker, *J. Vac. Sci. Technol. B*, **3**, 485 (1985).
19. R. H. Bruce, *Solid State Technol.*, 64 (Oct. 1981).

Phosphorous Vacancy Nearest Neighbor Hopping Induced Instabilities in InP Capacitors

I. Experimental

M. T. Juang, J. F. Wager, and J. A. Van Vechten*

Department of Electrical and Computer Engineering, Center for Advanced Materials Research, Oregon State University, Corvallis, Oregon 97331

ABSTRACT

Variable temperature bias-stress measurements were performed on n-type InP MIS capacitors. Two distinct activation energies at 40-50 meV and 1.1-1.2 eV were obtained over a temperature range of 100-350 K. These energies are consistent with the instability mechanisms of thermionic tunneling into native oxide traps and phosphorous vacancy nearest neighbor hopping (PVNNH). The estimated fraction of shift in these particular samples due to PVNNH varies both with stress time and with temperature from about 20% for short times at 300 K to about 80% for long times at 350 K.

The drain current of an InP metal insulator semiconductor field effect transistor (MISFET) is often observed to decrease as a function of time after the application of a positive gate bias which induces an accumulation of electrons in the channel. Various models have been proposed for this drain current drift (DCD) phenomena [see Ref. (1) for a critical review of proposed DCD models].

In this study, we have employed variable temperature bias-stress measurements (see the section on Experimental Procedure for a description of this technique) of InP MIS capacitors in order to determine the dominant DCD mechanisms from an analysis of the activation energy of the flatband shift. There are two advantages inherent in bias-stress measurements of MIS capacitors compared to DCD measurements of InP MISFET's. First, fabrication of the MIS capacitor requires fewer processing steps so that the interface chemistry can be precisely controlled and the electrical instabilities may be correlated to the interface drain current instabilities depend on both the carrier density and carrier mobility. Thus, interpretation of bias-stress measurements is more direct than that of DCD.

Two distinct activation energies at 40-50 meV and 1.1-1.2 eV were obtained from variable temperature bias-stress measurements over a temperature range of 100-350 K. The 40-50 meV activation energy dominates the flatband shift at low temperatures and is consistent with thermally activated tunneling of electrons from the InP conduction band into a discrete trap in the native oxide. An activation energy of 1.2 eV was predicted (2) for phosphorous vacancy nearest neighbor hopping (PVNNH) in which the channel electrons are captured by shallow acceptors that are created by the hopping of an In atom into a phosphorous vacancy.

PVNNH leads to DCD in the following manner. Consider an InP MISFET which has processing-induced P vacancies in the channel region under its gate. Nearest neigh-

DOCKET ALARM Find authenticated court documents without watermarks at docketalarm.com.